


[View Journal Online](#)
[View Article Online](#)

Exploring DNA-interaction and molecular structure of ruthenium/1,2-bis-(diphenylphosphino)ethane)-based complex

Victor Cardoso Campideli ^{1,†}, Jerica Margely Montilla-Suárez ^{1,†}, Tiago Almeida Silva ²,
 Dalila Chaves Sicupira ¹, Katia Mara Oliveira ³ and Rodrigo Souza Correa ^{1,*}

¹ Departamento de Química, Universidade Federal de Ouro Preto (UFOP), Ouro Preto, MG, 35400-000, Brazil

² Departamento de Química, Universidade Federal de Viçosa (UFV), Viçosa, MG, 36570-900, Brazil

³ Instituto de Química, Universidade de Brasília (UnB), Brasília, DF, 70910-900, Brazil


* Corresponding author at: Departamento de Química, Universidade Federal de Ouro Preto (UFOP), Ouro Preto, MG, 35400-000, Brazil.

† These authors contributed equally.

e-mail: rodrigocorrea@ufop.edu.br (R.S. Correa).

RESEARCH ARTICLE



 10.5155/eurjchem.14.2.193-201.2402

Received: 24 December 2022

Received in revised form: 29 January 2023

Accepted: 11 February 2023

Published online: 30 June 2023

Printed: 30 June 2023

KEYWORDS

Viscosity
 DNA interaction
 Crystal structure
 Ru/dppe complex
 UV-Vis spectroscopy
 Square-wave voltammetry

ABSTRACT

The mixture of *cis* and *trans*-[RuCl₂(dppe)₂] (dppe: 1,2-bis-(diphenylphosphino)ethane) was prepared and the interaction with CT-DNA was evaluated by several methods, including UV-Vis DNA spectroscopic titration, viscosity, and electrochemical studies. Investigation suggests that [RuCl₂(dppe)₂] interacts moderately with CT-DNA. Interestingly, the *cis*- and *trans*-isomers interact differently with DNA, as proved by the square-wave voltammetry studies. Finally, the crystal structure of *trans*-[RuCl₂(dppe)₂]Cl was obtained from an electrochemical solution and studied in detail, which presents a distorted octahedral geometry and interatomic parameters different from those found in the *trans*-[RuCl₂(dppe)₂] complex. Crystal data for C₅₂H₄₈Cl₄P₄Ru: triclinic, space group *P*-1 (no. 2), *a* = 9.240(3) Å, *b* = 10.9290(18) Å, *c* = 11.993(3) Å, α = 78.707(11)°, β = 86.712(13)°, γ = 82.598(13)°, *V* = 1177.1(5) Å³, *Z* = 1, *T* = 293(2) K, μ (MoK α) = 0.732 mm⁻¹, *D*_{calc} = 1.467 g/cm³, 8434 reflections measured (6.934° ≤ 2 θ ≤ 51.986°), 4607 unique (*R*_{int} = 0.0973, *R*_{sigma} = 0.1171) which were used in all calculations. The final *R*₁ was 0.0537 (*I* > 2 σ (*I*)) and *wR*₂ was 0.1347 (all data).

Cite this: *Eur. J. Chem.* 2023, 14(2), 193-201

Journal website: www.eurjchem.com

1. Introduction

Cancer is the replication of tumor cells (genetically modified) and can occur in several different ways in the human body. One of these disease treatments consists of the use of anticancer drugs, known as chemotherapeutic agents, in which one of the mechanisms of action is to interact with DNA altering its structure, leading to cell death, modulation of transcription, or interfering in replication to prevent the rapid proliferation of cancer cells in the body [1]. In recent years, many studies have been conducted based on metallodrug development based on the interaction of metal complexes with DNA, to understand the mechanism of action [2].

Since the discovery of *cis*-platin as a metallodrug in the late 1960s, scientists have been looking for new coordination compounds to fight cancer [3]. There are many platinum-based complexes with high biological activity. However, side effects and resistance have led many researchers to explore other non-platinum compounds, such as ruthenium, which has been widely studied in recent years [4,5].

DNA may be a target for anticancer metallodrugs and recent studies have used several compounds that interact with DNA as useful tools to visualise DNA damage [5,6]. Many assays are powerful tools for determining the mechanism of action of new molecules and can be crucial to the discovery of the next generation of DNA-binding anticancer metallodrugs. The covalent bond between metallodrug-DNA is an irreversible chemical bond that causes complete inhibition of DNA processes leading to cell death, as is suggested to occur with *cis*-platin [7]. On the other hand, the non-covalent bond is almost reversible or reversible, in which metallodrugs interact with DNA weakly or moderately. Generally, there are three main modes of non-covalent interactions, which include electrostatic interaction, groove binding, and intercalative binding [8-10]. To determine the type of metallodrug-DNA interactions, many techniques can be used, including cyclic voltammetry (CV) and square wave voltammetry (SWV) [11], nuclear magnetic resonance (NMR) [12], UV-visible and fluorescence titration studies [13], viscosity [14], circular dichroism (CD) and the Hoechst 33 258 staining assay [15], capillary electrophoresis (CE) [16] and atomic force microscopy (AFM) [17].

In recent years, there has been interest in the discovery and understanding of the cytotoxic activity of compounds based on ruthenium / phosphine and exploring their interaction with DNA as a possible target [18-20]. The complex studied in the present report is identified as $[\text{RuCl}_2(\text{dppe})_2]$, in which dppe is 1,2-bis-(diphenylphosphino)ethane and a mixture of *cis* and *trans* isomers of $[\text{RuCl}_2(\text{dppe})_2]$ has been used. The $[\text{RuCl}_2(\text{dppe})_2]$ complex was previously used as a precursor to obtain new active compounds [21,22]. In this study, the $[\text{RuCl}_2(\text{dppe})_2]$ /DNA interaction was investigated using viscosity, UV-vis DNA titration, and square-wave voltammetry. In addition, the crystal structure of *trans*- $[\text{RuCl}_2(\text{dppe})_2]\text{Cl}$ is reported.

2. Experimental

2.1. Synthesis of the *cis*- $[\text{RuCl}_2(\text{DMSO})_4]$ complex

The *cis*- $[\text{RuCl}_2(\text{DMSO})_4]$ complex was synthesised by refluxing 0.5 g (2.41 mmol) of $\text{RuCl}_3 \cdot x\text{H}_2\text{O}$ in dimethyl sulfoxide (DMSO) (5 mL) for 15 minutes. The reaction mixture was cooled to room temperature and acetone (20 mL) was added to form the yellow precipitate, which was washed with acetone and ethyl ether and vacuum-dried.

2.2. Synthesis of *cis*- and *trans*- $[\text{RuCl}_2(\text{dppe})_2]$

The mixture of *cis*- and *trans*- $[\text{RuCl}_2(\text{dppe})_2]$ complexes was obtained according to the methodology described by Bautista et al. [23]. For this, *cis*- $[\text{RuCl}_2(\text{DMSO})_4]$ 0.5 g (1.03 mmol) and 1,2-bis(diphenylphosphino)ethylene (dppe) 0.94 g (2.37 mmol) were added to 20 mL of dichloromethane. The reaction mixture was kept stirring for 5 hours and then the volume of the solution was reduced to approximately 3 mL. Subsequently, hexane was added to form a pale-yellow precipitate, which presents the mixture of complexes *cis* and *trans*- $[\text{RuCl}_2(\text{dppe})_2]$.

2.3. UV-vis DNA spectroscopic titration

The DNA solution was prepared by adding approximately 1.2 mg of CT-DNA (*Calif Thymus*) in approximately 1000 μL of tris-HCl buffer (4.5 mmol of Tris HCl, 0.5 mmol of Tris base and 50 mmol of NaCl) at a pH of 7.4. The exact concentration of CT-DNA was provided by spectroscopy in the UV-vis region. In a cuvette containing only a buffer solution (2000 μL), 80 μL of CT-DNA solution was added and the measurement was performed on the equipment. It is known that the molar absorptivity of CT-DNA at 260 nm is $6600 \text{ mol}^{-1} \cdot \text{cm}^{-1} \cdot \text{L}$. Therefore, knowing the absorbance and molar absorptivity at 260 nm and the optical path of the cuvette ($b = 1 \text{ cm}$), the concentration of CT-DNA was determined using the Lambert-Beer law:

$$A_{260} = \varepsilon_{260} \times b \times c \quad (1)$$

Titration were performed using two cuvettes: In cuvette I, corresponding to the blank, 1700 μL of tris buffer and 300 μL of DMSO were added, and in cuvette II, 1700 μL of tris buffer were added and 300 μL of the solution of the ruthenium complex in DMSO (in a concentration that does not exceed the Lambert-Beer Law). Then successive additions of 10 μL of CT-DNA were performed in the two cuvettes. The solutions were homogenised for about half a minute and then the spectrum was recorded.

The interaction constant (K_b) with DNA was determined based on the absorption maximum for each complex, using equation (2):

$$\frac{[DNA]}{(\varepsilon_a - \varepsilon_f)} = \frac{[DNA]}{(\varepsilon_b - \varepsilon_f)} + \frac{1}{[K_b(\varepsilon_b - \varepsilon_f)]} \quad (2)$$

where: ε_a , ε_f , ε_b are the $A_{\text{obsd}}/[\text{Complex}]$, the molar extinction coefficient of the free and bounded metal complexes, respectively.

2.4. DNA interaction by electrochemical studies

The electrochemical characterization of the $[\text{RuCl}_2(\text{dppe})_2]$ complex was performed using a Potentiostat/Galvanostat Autolab model 302N, using a glass cell and a three-electrode system, in which platinum was used as the working and auxiliary electrode and Ag/AgCl (3.0 mol/L KCl) as the reference electrode. The $[\text{RuCl}_2(\text{dppe})_2]$ complex solution was prepared in dichloromethane (0.1 mol/L of tetrabutyl ammonium perchlorate (PTBA)) at a concentration of 2×10^{-4} mol/L. Cyclic voltammograms were recorded in the range of 0 to +1.6 V at different scan rates (10-100 mV/s). To assess the interaction of the $[\text{RuCl}_2(\text{dppe})_2]$ complex with CT-DNA, the square-wave voltammetry technique was used. A system of three electrodes was used, with the glassy carbon working electrode, Ag/AgCl (3.0 mol/L KCl) as a reference electrode and as the auxiliary electrode, a platinum plate. The $[\text{RuCl}_2(\text{dppe})_2]$ complex was prepared in a mixture of Tris-HCl buffer (4.5 mM Tris-HCl, 0.5 mM Tris-base and 0.1 mol/L NaCl, pH = 7.4) with 40% DMSO at a concentration of 1×10^{-4} M. First, the voltammetric profile of the complex was recorded and then successive 10 μL aliquots of a CT-DNA solution (4.67×10^{-3} M) were added to the complex solution. With each addition of CT-DNA, the system was shaken for a period of 5 min and then the voltammogram was recorded.

2.5. Viscosity

To determine the changes that occur in the viscosity of a CT-DNA solution, solutions with different CT-DNA:metal complex molar ratios of 0.2, 0.3, 0.4, 0.5 and 0.6 were prepared. Viscosity measurements were made using an Oswald viscometer in the thermostatic water bath at 25 °C. Thus, keeping the concentration of CT-DNA constant (3.66×10^{-3} mol/L), a viscosity ratio η can be obtained from the following equation:

$$\eta = \frac{t - t_0}{t_0} \quad (3)$$

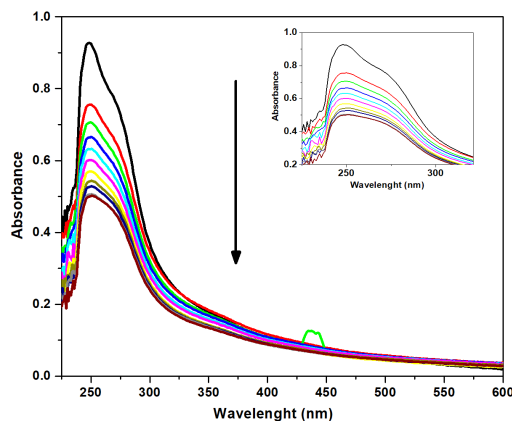
where: t is the elution time of the solution CT-DNA:metal complex, and t_0 is the elution time of free DNA. With the data obtained, it is possible to construct a graph of the relative viscosity vs. $[\text{DNA}]/[\text{complex}]$, and to evaluate the possible changes in the viscosity of CT-DNA, in the presence of ruthenium complex.

2.6. X-ray crystallography study

Single crystals of $[\text{RuCl}_2(\text{dppe})_2]\text{Cl}$ were obtained at room temperature by slow solvent evaporation of the electrochemical solution. The X-ray diffraction experiment was carried out at room temperature on an Enraf-Nonius Kappa-CCD diffractometer using the MoK α radiation ($\lambda = 0.71073 \text{ \AA}$) monochromated with graphite. The crystal structure of *trans*- $[\text{RuCl}_2(\text{dppe})_2]\text{Cl}$ was solved by the direct method and refined using the SHELXS-97 and SHELXL-97 programmes (Table 1) [24], respectively. Absorption corrections were carried out using the Gaussian method, and all non-hydrogen atoms of *trans*- $[\text{RuCl}_2(\text{dppe})_2]\text{Cl}$ were located and refined with anisotropic thermal parameters. The C-H aromatic hydrogen atoms were added with C-H distance, fixed at 0.93 \AA , and refined with fixed displacement parameters [$U_{\text{iso}}(\text{H}) = 1.2 U_{\text{eq}}(\text{Csp}^2)$].

Table 1. Crystal data and structure refinement for complex *trans*-[RuCl₂(dppe)₂]Cl.

Empirical formula	C ₅₂ H ₄₈ Cl ₄ P ₄ Ru
Formula weight (g/mol)	1039.65
Temperature (K)	293(2)
Crystal system	Triclinic
Space group	<i>P</i> -1
<i>a</i> , (Å)	9.240(3)
<i>b</i> , (Å)	10.9290(18)
<i>c</i> , (Å)	11.993(3)
α (°)	78.707(11)
β (°)	86.712(13)
γ (°)	82.598(13)
Volume (Å ³)	1177.1(5)
<i>Z</i>	1
ρ _{calc} (g/cm ³)	1.467
μ (mm ⁻¹)	0.732
F(000)	532.0
Crystal size (mm ³)	0.18 × 0.08 × 0.03
Radiation	MoKα (λ = 0.71073)
2θ range for data collection (°)	6.934 to 51.986
Index ranges	-11 ≤ <i>h</i> ≤ 11, -13 ≤ <i>k</i> ≤ 13, -14 ≤ <i>l</i> ≤ 14
Reflections collected	8434
Independent reflections	4607 [R _{int} = 0.0973, R _{sigma} = 0.1171]
Data/restraints/parameters	4607/0/277
Goodness-of-fit on F ²	0.956
Final R indexes [I ≥ 2σ (I)]	R ₁ = 0.0537, wR ₂ = 0.1222
Final R indexes [all data]	R ₁ = 0.0795, wR ₂ = 0.1347
Largest diff. peak/hole (e.Å ⁻³)	0.73/-0.95

**Figure 1.** *cis*- and *trans*-isomers of complex [RuCl₂(dppe)₂].**Figure 2.** Absorption spectrum in the UV-Vis region of the complex [RuCl₂(dppe)₂] (isomers *cis* / *trans*), in the concentration 1.5 × 10⁻³ mol/L, in the presence of successive additions of rates of CT-DNA (2.05 × 10⁻³ mol/L), in buffer Tris-HCl (pH = 7.4) and 10% of DMSO.

The hydrogen of methylene groups of dppe was also set as isotropic with a thermal parameter 20% greater than the equivalent isotropic displacement parameter of the atom to which each one was bonded, and C-H bond lengths were fixed at 0.97 Å. For structure representation, the Mercury 4.0 programme was used [25].

3. Results and discussion

The mixture of *trans*- and *cis*-[RuCl₂(dppe)₂] complexes was obtained from the precursor *cis*-[RuCl₂(DMSO)₄] by replacing the four DMSO ligands with two diphosphine dppe (1,2-*bis*-(diphenylphosphino)ethane) ligands, as shown in Figure 1. The mixture of isomers was confirmed by ³¹P{¹H} NMR, in which one singlet at δ 44 ppm is related to isomer *trans* and two

triplets at δ 50.29 and 37.35 ppm (²*J*_{P-P} = 19.6 Hz) belong to isomer *cis*.

3.1. UV-Vis DNA spectroscopic titration and viscosity

First, spectrophotometric titrations were performed to evaluate the interaction of the [RuCl₂(dppe)₂] complex with CT-DNA. This technique is widely used to determine the complex-DNA affinity, in which the binding constant values (*K_b*) can indicate a high, moderate or weak interaction [26]. The UV-Vis spectrum for the [RuCl₂(dppe)₂] complex was investigated in the region between 200 and 600 nm. In Figure 2, it is possible to observe that the spectra of the mixture of *cis*- and *trans*-[RuCl₂(dppe)₂] complex decrease with CT-DNA addition, resulting in a hypochromism.

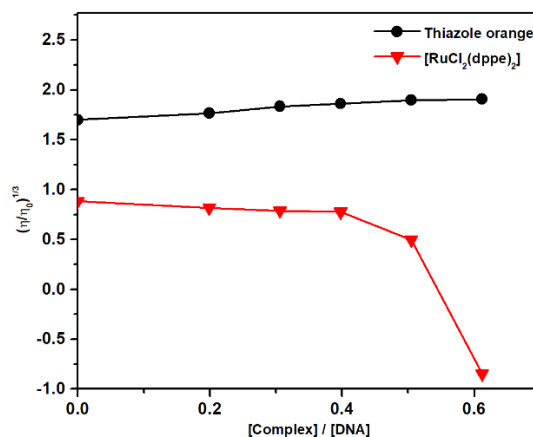


Figure 3. Relative viscosity vs [DNA]/[complex], of thiazole orange and the complex $[\text{RuCl}_2(\text{dppe})_2]$ at a concentration 1.5×10^{-3} mol/L, in the presence of successive additions of CT-DNA ratios (3.66×10^{-3} mol/L), in Tris-HCl buffer (pH = 7.4) and DMSO.

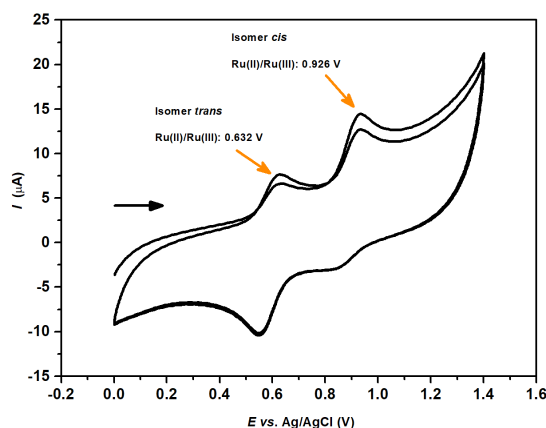


Figure 4. Cyclic voltammogram of the complex $[\text{RuCl}_2(\text{dppe})_2]$ (isomer *cis* e *trans*), in concentration 2×10^{-4} mol/L in 0.1 mol/L PTBA, in CH_2Cl_2 . Scan rate = 50 mV/s.

The initial spectrum (black) corresponds to the free complex (in the absence of DNA), while the other data were obtained after successive additions of 10 μL of CT-DNA to the complex solution. The K_b value was calculated from the absorption band (λ_{max}) at about 250 nm to the complex, and the K_b value is $3.9 \times 10^4 \text{ M}^{-1}$, revealing a moderate interaction compared with other metal complexes reported in the literature [27,28].

In addition, to better understand the interaction between the ruthenium complex and CT-DNA, viscosity measurements were performed. Intercalation and groove-binding interactions have been reported to contribute to an increase in viscosity, whereas covalent binding can cause a decrease in the relative viscosity of CT-DNA [29].

When the concentration of the ruthenium complex increases, the relative viscosity of CT-DNA decreases (Figure 3). For comparison, DNA viscosity was performed using a DNA intercalator, known as thiazole orange [30], which increases DNA viscosity in all molar additions studied. Therefore, a different curve profile for the ruthenium complex compared with thiazole orange may suggest that the complex does not act as a DNA intercalator.

3.2. Electrochemical and DNA interaction study by square wave voltammetry

The complex $[\text{RuCl}_2(\text{dppe})_2]$ was characterized using cyclic voltammetry (Figure 4). This technique was used because of its sensitivity to redox processes. Cyclic voltammograms were

investigated in the range of 0 to +1.6 V at different scan rates, and the recorded cyclic voltammograms in the scan rate range of 10-100 mV/s can be seen in Figure 5.

In the cyclic voltammogram shown in Figure 4, the electrochemical profile of the $[\text{RuCl}_2(\text{dppe})_2]$ complex presents two oxidation processes Ru(II)/Ru(III) at +0.632 V and +0.926 V, referring to the *cis*- and *trans*-isomers of the $[\text{RuCl}_2(\text{dppe})_2]$ complex, respectively.

The oxidation potential Ru(II)/Ru(III) for the *cis* isomer occurs in a more positive region (+0.926 V) when compared to the *trans* isomer (+0.632 V), indicating that in *cis*-configuration ruthenium is more deficient in electron density, requiring a higher potential for oxidation of the metal. The redox potential for the *cis*-isomer occurs at a higher potential than that of the *trans*-isomer as a result of the increase in the back-donation of ruthenium to the phosphorus atom in the *cis*-isomer. This behaviour occurs because phosphorus *trans* to phosphorus increases the *trans* cooperative effect, lowering the redox potential, which agrees with expected by Sullivan and Meyer [31]. From the cyclic voltammograms obtained at different scan rates, linear relationships between anodic peak current and the square root of the scan rate (I_p vs. $v^{1/2}$) shown in Figure 5) were obtained for the oxidation peak of the *cis* and *trans* isomers, showing that both redox processes were controlled only by diffusion.

The electrochemical response of the complex can change in the presence of DNA. Intercalation interactions lead to the potential shift to positive values as a result of the increase in the diffusion coefficient caused by the DNA molecule.

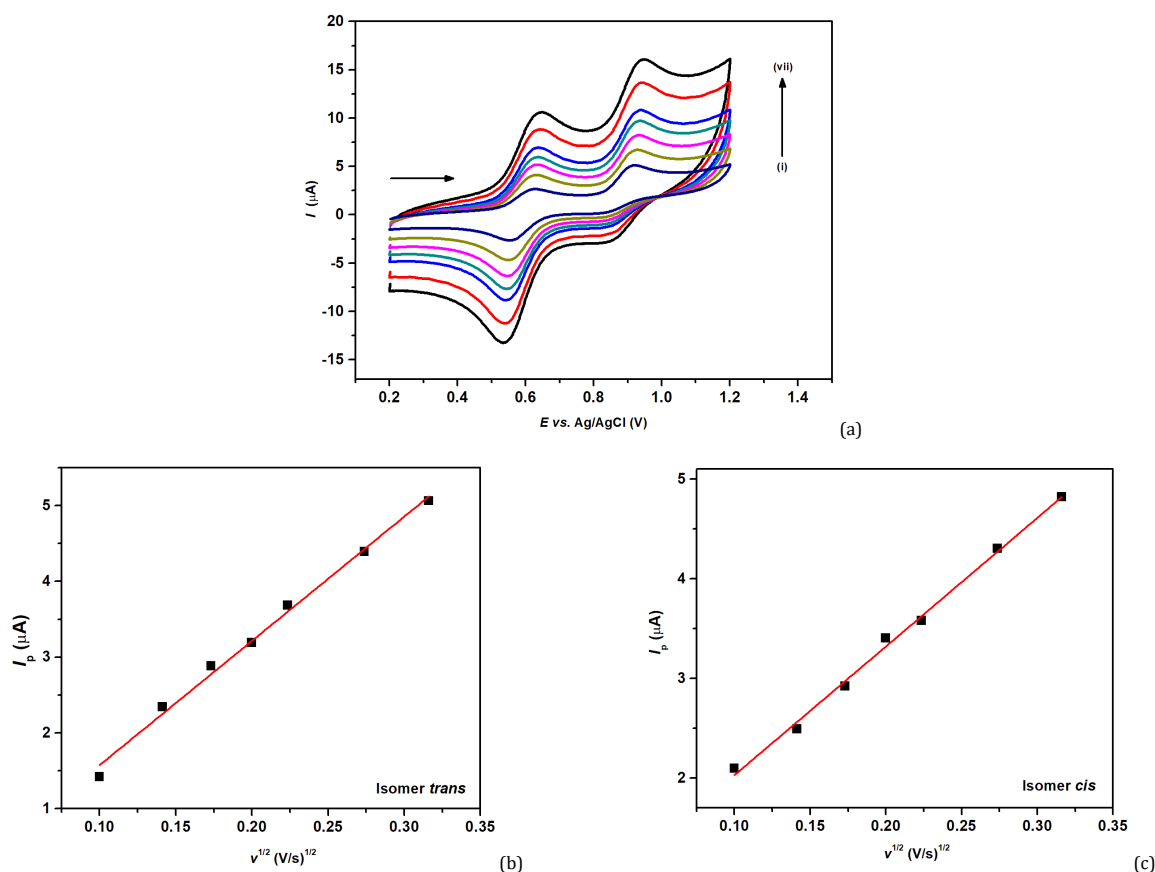


Figure 5. (a) Cyclic voltammogram of the complex $[\text{RuCl}_2(\text{dppe})_2]$ (isomer *cis* and *trans*), at concentration 2×10^{-4} mol/L in 0.1 mol/L PTBA, in CH_2Cl_2 at different scan rates: (i) 10 mV/s; (ii) 20 mV/s; (iii) 30 mV/s; (iv) 40 mV/s; (v) 50 mV/s; (vi) 75 mV/s and (vii) 100 mV/s. (b, c) Graph of I_p vs. $v^{1/2}$ obtained for the anodic peak of the isomer *trans* and isomer *cis*.

On the contrary, electrostatic interactions promote a displacement of the potential to more negative values, since electrons are transferred from DNA to the complex. Covalent interactions, when new species are generated, lead to the appearance of new redox processes or the disappearance of existing processes. Interactions between the DNA grooves may not promote significant changes in potential values, but they do change the number of complexes available that can undergo redox reactions, as in other modes of interaction, affecting the intensity of electrochemical processes [13,32]

Electrochemical study of the interaction with CT-DNA with the mixture of *cis*- and *trans*- $[\text{RuCl}_2(\text{dppe})_2]$ complexes was performed using SWV. This technique was used because of its high sensitivity to redox processes and reaction formation, which is greater than that of the cyclic voltammetry technique. Figure 6 shows the recorded voltammetric profile of the complex with successive 10 μL aliquots of a CT-DNA solution.

After adding different concentrations of CT-DNA to the solution containing the mixture of *cis* and *trans*- $[\text{RuCl}_2(\text{dppe})_2]$ complexes (Figure 6), a significant current decrease was observed in the Ru(II)/Ru(III) redox process, indicating that complex/DNA interactions are occurring. In the *cis*-isomer (Figure 6), the current of the Ru(II)/Ru(III) redox process decreases and the potential does not change; this behaviour may indicate an interaction between the DNA grooves. On the other hand, analysing the Ru(II)/Ru(III) redox process for the *trans*-isomer after successive CT-DNA additions (Figure 6), it is possible to observe that the potential shifted to the most positive region and a subsequent increase in the peak current, in the case of the latest CT-DNA additions. This result indicates that the *trans*-isomer may be interacting with CT-DNA through intercalation or even through covalence, different from the

behaviour observed in the *cis*-isomer of the $[\text{RuCl}_2(\text{dppe})_2]$ complex.

To investigate whether the redox potential changes due to the dilution effect, we recorded a square-wave voltammogram of the complex adding only Tris-HCl buffer (without DNA), and no significant changes were observed. Thus, the peak current decrease occurs through DNA interaction.

3.3. Single crystal X-ray diffraction of complex *trans*- $[\text{RuCl}_2(\text{dppe})_2]\text{Cl}$

The electrochemical solution produced orange crystals after one week. The crystals were analysed by single crystal X-ray diffraction and resulted in the *trans*- $[\text{RuCl}_2(\text{dppe})_2]\text{Cl}$ complex (Figure 7). We highlight that in the crystal structure the metal center is in Ru^{3+} oxidation state, thus this is an unpublished structure, given that in the literature only the *trans*- $[\text{RuCl}_2(\text{dppe})_2]$ was reported and the metal center is Ru^{2+} .

The X-ray crystallographic studies confirm the presence of two dppe as bidentate ligands and two chlorido ligands in a *trans*-configuration. In the structure, the Ru atom is located on an inversion centre; thus, a half-molecule is observed in the asymmetric unit. The complex presents a slightly distorted octahedral geometry, as highlighted by the bond angles around the metal centres (Table 2). In the complex structure, the Cl1-Ru1-P1 ($98.53(4)/81.47(4)^\circ$) and Cl1-Ru1-P2 ($91.74(4)/88.26(4)^\circ$) bond angles are close to 90° , and the P1-Ru1-P2 ($99.03(4)/80.97(4)^\circ$) bond angle is far from the expected value of 90° due to the tension of the five-membered chelate rings of the dppe ligand. The Cl1-Ru1-Cl2 bond angle adopting a *trans*-configuration is 180° .

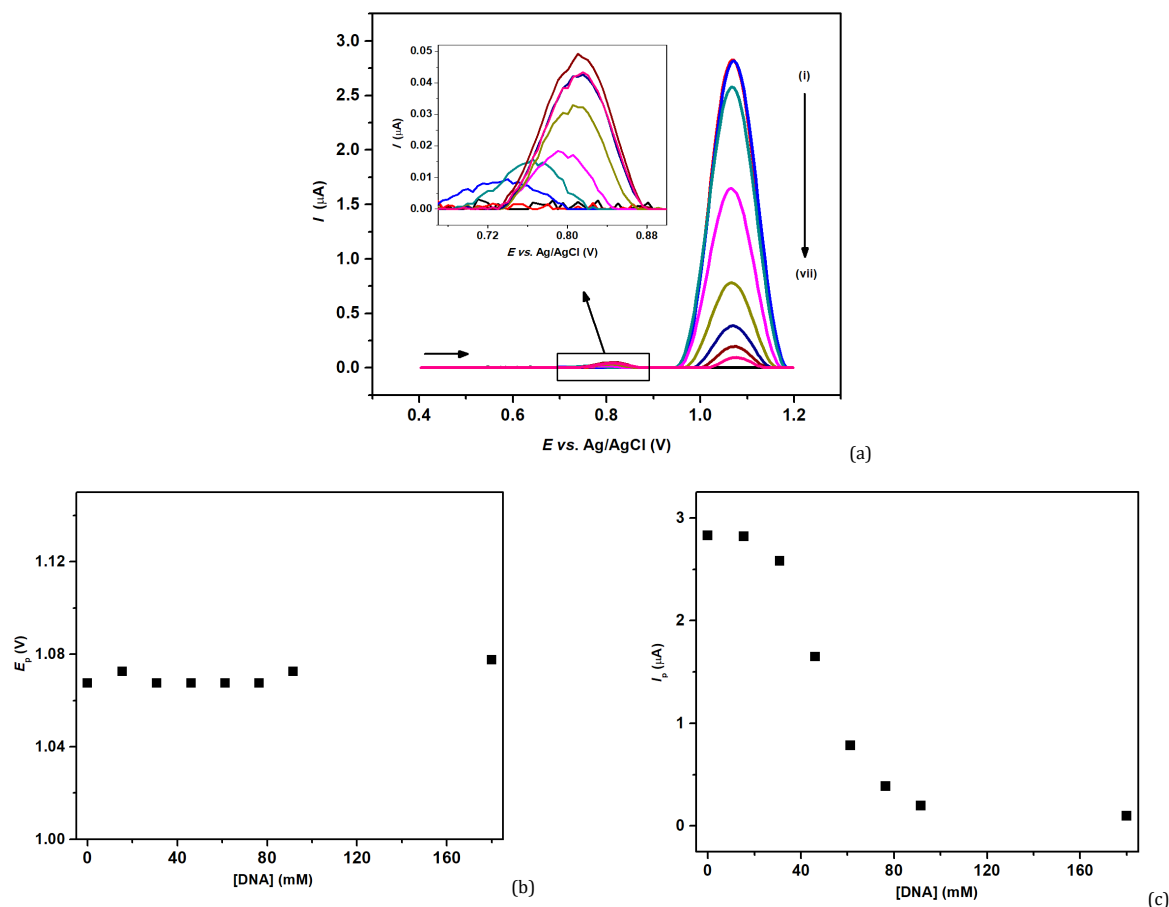


Figure 6. (a) Square wave voltammograms obtained in buffer Tris-HCl (pH = 7.4)-40% (v/v) DMSO containing (i) $[\text{RuCl}_2(\text{dppe})_2]$ 100 μM ; (ii) $[\text{RuCl}_2(\text{dppe})_2]$ 100 μM + DNA 15.5 μM ; (iii) $[\text{RuCl}_2(\text{dppe})_2]$ 100 μM + CT-DNA 30.9 μM ; (iv) *cis*- $[\text{RuCl}_2(\text{dppe})_2]$ 100 μM + CT-DNA 46.2 μM ; (v) $[\text{RuCl}_2(\text{dppe})_2]$ 100 μM + CT-DNA 61.4 μM ; (vi) $[\text{RuCl}_2(\text{dppe})_2]$ 100 μM + CT-DNA 76.5 μM ; (vii) $[\text{RuCl}_2(\text{dppe})_2]$ 100 μM + CT-DNA 91.6 μM and (viii) $[\text{RuCl}_2(\text{dppe})_2]$ 100 μM + CT-DNA 180.0 μM . Parameters SWV: Frequency (f) = 20 Hz, Amplitude (A) = 50 mV, and potential increment (ΔE_s) = 5 mV. (b) Graphs of peak potential *versus* concentration CT-DNA (E_p vs. [CT-DNA]) and (c) Peak current *versus* concentration CT-DNA (I_p vs. [CT-DNA]).

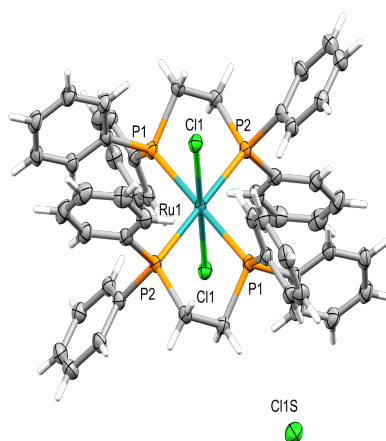


Figure 7. Crystal structure of $[\text{RuCl}_2(\text{dppe})_2]\text{Cl}$ with ellipsoids drawn at 30% probability.

Furthermore, it is observed that the bond lengths of Ru-P and Ru-Cl are in agreement with the values reported for Ru(III) complexes [33,34]. In the literature, four crystal structures containing the complex *trans*- $[\text{RuCl}_2(\text{dppe})_2]$ were reported. A solvent-free structure of *trans*- $[\text{RuCl}_2(\text{dppe})_2]$ [35] and three other crystalline forms containing one dichloromethane solvate [36], one chloroform solvate, and one tetrahydrofuran solvate [37].

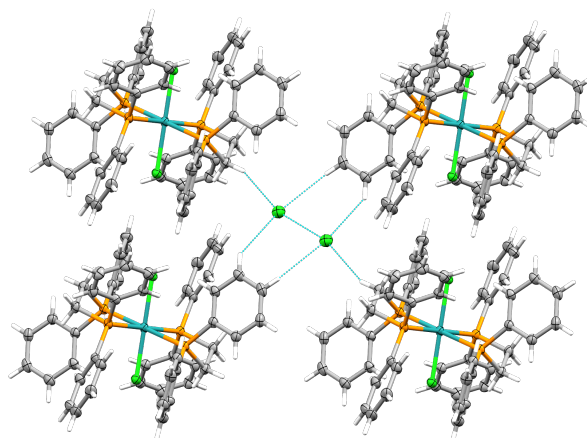
When the structure of *trans*- $[\text{RuCl}_2(\text{dppe})_2]\text{Cl}$ is compared with *trans*- $[\text{RuCl}_2(\text{dppe})_2]$ [36], many differences can be

observed. In *trans*- $[\text{RuCl}_2(\text{dppe})_2]\text{Cl}$ the Ru-Cl distance is 2.3310(12) Å, while the *trans*- $[\text{RuCl}_2(\text{dppe})_2]$ is slightly larger [2.436(1) Å], which is expected for a low-charged metal. On the other hand, the Ru^{III}-P bond distance for $[\text{RuCl}_2(\text{dppe})_2]$ is 2.369(1) Å [36] and 2.3811(13) Å [37], while in the structure reported here, the Ru^{III}-P bond distance is also slightly larger [Ru1-P1 = 2.4587(11) and Ru1-P2 = 2.4374(11) Å], this aspect may be explained because, in the Ru(III) complex, the Ru-ligand back-donation decreases, thus, Ru-P bond is slightly weaker.

Table 2. Bond lengths and angles for *trans*-[RuCl₂(dppe)₂]Cl*.

Bond lengths							
Atom	Atom	Length (Å)	Atom	Atom	Length (Å)		
Ru1	P2 ¹	2.4374(11)	C212	C213	1.390(6)		
Ru1	P2	2.4374(11)	C111	C116	1.386(6)		
Ru1	P1 ¹	2.4586(11)	C111	C112	1.398(6)		
Ru1	P1	2.4587(11)	C126	C125	1.396(6)		
Ru1	Cl1	2.3310(12)	C124	C125	1.369(7)		
Ru1	Cl1 ¹	2.3310(12)	C124	C123	1.367(6)		
P2	C211	1.825(4)	C122	C123	1.389(6)		
P2	C221	1.823(4)	C226	C225	1.383(6)		
P2	C231	1.853(4)	C116	C115	1.382(6)		
P1	C121	1.840(4)	C213	C214	1.357(7)		
P1	C111	1.816(4)	C216	C215	1.383(6)		
P1	C131	1.833(4)	C112	C113	1.382(6)		
C211	C212	1.380(6)	C215	C214	1.383(7)		
C211	C216	1.400(6)	C114	C115	1.379(7)		
C221	C226	1.385(6)	C114	C113	1.377(7)		
C221	C222	1.406(6)	C225	C224	1.371(8)		
C231	C131	1.524(5)	C223	C224	1.372(8)		
C121	C126	1.381(5)	C223	C222	1.379(6)		
C121	C122	1.384(6)					
Bond angles							
Atom	Atom	Atom	Angle (°)	Atom	Atom	Atom	Angle (°)
P2 ¹	Ru1	P2	180.0	C226	C221	C222	118.2(4)
P2 ¹	Ru1	P1	99.03(4)	C222	C221	P2	121.6(3)
P2	Ru1	P1	80.97(4)	C131	C231	P2	110.7(3)
P2	Ru1	P1 ¹	99.03(4)	C126	C121	P1	122.8(3)
P2 ¹	Ru1	P1 ¹	80.97(4)	C126	C121	C122	119.0(4)
P1 ¹	Ru1	P1	180.0	C122	C121	P1	117.9(3)
Cl1	Ru1	P2 ¹	91.74(4)	C211	C212	C213	120.5(4)
Cl1 ¹	Ru1	P2	91.74(4)	C116	C111	P1	119.2(3)
Cl1	Ru1	P2	88.26(4)	C116	C111	C112	118.3(4)
Cl1 ¹	Ru1	P2 ¹	88.26(4)	C112	C111	P1	122.4(3)
Cl1 ¹	Ru1	P1 ¹	81.47(4)	C231	C131	P1	107.0(3)
Cl1	Ru1	P1 ¹	98.53(4)	C121	C126	C125	120.2(4)
Cl1	Ru1	P1	81.47(4)	C123	C124	C125	120.4(4)
Cl1 ¹	Ru1	P1	98.53(4)	C121	C122	C123	120.5(4)
Cl1 ¹	Ru1	Cl1	180.0	C225	C226	C221	121.3(5)
C211	P2	Ru1	118.35(13)	C115	C116	C111	121.5(4)
C211	P2	C231	103.6(2)	C124	C125	C126	119.9(4)
C221	P2	Ru1	118.74(15)	C124	C123	C122	119.9(5)
C221	P2	C211	102.89(19)	C214	C213	C212	120.6(5)
C221	P2	C231	103.56(18)	C215	C216	C211	121.1(5)
C231	P2	Ru1	107.79(13)	C113	C112	C111	120.0(5)
C121	P1	Ru1	124.86(13)	C216	C215	C214	119.2(5)
C111	P1	Ru1	117.70(14)	C113	C114	C115	120.0(4)
C111	P1	C121	102.02(18)	C114	C115	C116	119.5(5)
C111	P1	C131	107.09(19)	C224	C225	C226	119.5(5)
C131	P1	Ru1	103.19(14)	C224	C223	C222	120.5(5)
C131	P1	C121	99.5(2)	C225	C224	C223	120.5(4)
C212	C211	P2	121.6(3)	C223	C222	C221	119.9(4)
C212	C211	C216	118.2(4)	C213	C214	C215	120.5(5)
C216	C211	P2	120.2(3)	C114	C113	C112	120.7(5)
j	C221	P2	120.2(3)				

* Symmetry code: 1-x, 2-y, -z.

**Figure 8.** C-H...Cl hydrogen bonding and Cl...Cl halogen bond, stabilizing the crystal structure of the complex *trans*-[RuCl₂(dppe)₂]Cl.

The crystal structure of *trans*-[RuCl₂(dppe)₂]Cl presents non-classical C-H...Cl₁s hydrogen bonding, keeping the counter-ion caged (Figure 8). The C-H...Cl intermolecular contacts are around 2.8 Å. Furthermore, the complex presents an intermolecular Cl...Cl halogen bond at 3.123 Å, which is consistent with values reported elsewhere [38].

4. Conclusions

In summary, the interaction with DNA of *cis* and *trans* isomers of the complex [RuCl₂(dppe)₂] was investigated. UV-Vis and viscosity analysis showed that the *cis*- and *trans*-isomer mixtures exhibit moderate interaction with DNA. Interestingly, DNA interaction by square wave voltammetric indicates that the interaction of *cis*-isomer may occur by DNA grooves, while the complex *trans*-[RuCl₂(dppe)₂] probably interacts with DNA by intercalation or by covalence. Finally, the crystal structure of the *trans*-[RuCl₂(dppe)₂]Cl complex was presented and compared with the *trans*-[RuCl₂(dppe)₂] complex. This study contributes to a better understanding of complex/DNA interaction, mainly, allowing identification of two different DNA interaction modes by using square wave voltammograms.

Acknowledgements

We would like to thank Conselho Nacional de Desenvolvimento Científico e Tecnológico (CNPq), Coordenação de Aperfeiçoamento de Pessoal de Nível Superior (CAPES), and Fundação de Amparo à Pesquisa do Estado de Minas Gerais (FAPEMIG) for the financial support. Jerica Margely Montilla-Suárez thanks the Universidade Federal de Ouro Preto for master's fellowship. The authors thank Professor Javier Ellena for crystallographic facilities and Professor Alzir A. Batista for providing the ruthenium salt.

Supporting information

CCDC-2232620 contains the supplementary crystallographic data for this paper. These data can be obtained free of charge via <https://www.ccdc.cam.ac.uk/structures/>, or by e-mailing data_request@ccdc.cam.ac.uk, or by contacting The Cambridge Crystallographic Data Centre, 12 Union Road, Cambridge CB2 1EZ, UK; fax: +44(0)1223-336033.

Disclosure statement

Conflict of interest: The authors declare that they have no known competing financial interests or personal relationships that could appear to influence the work reported in this paper.
Sample availability: Samples of the compound are available from the author.

CRedit authorship contribution statement

Conceptualization: Victor Cardoso Campideli, Jerica Margely Montilla-Suárez, Rodrigo Souza Corrêa; Methodology: Victor Cardoso Campideli, Jerica Margely Montilla-Suárez, Tiago Almeida Silva, Dalila Chaves Sicupira, Katia Mara Oliveira, Rodrigo Souza Correa; Software: Katia Mara Oliveira, Rodrigo Souza Correa; Validation: Tiago Almeida Silva, Dalila Chaves Sicupira, Katia Mara Oliveira, Rodrigo Souza Correa; Formal Analysis: Victor Cardoso Campideli, Jerica Margely Montilla-Suárez, Tiago Almeida Silva; Resources: Dalila Chaves Sicupira, Katia Mara Oliveira, Rodrigo Souza Correa; Data Curation: Victor Cardoso Campideli, Jerica Margely Montilla-Suárez, Katia Mara Oliveira; Writing - Original Draft: Victor Cardoso Campideli, Jerica Margely Montilla-Suárez, Katia Mara Oliveira, Rodrigo Souza Correa; Writing - Review and Editing: Katia Mara Oliveira, Rodrigo Souza Correa; Visualization: Katia Mara Oliveira, Rodrigo Souza Correa; Funding acquisition: Rodrigo Souza Correa; Supervision: Katia Mara Oliveira, Rodrigo Souza Correa; Project Administration: Dalila Chaves Sicupira, Katia Mara Oliveira, Rodrigo Souza Correa.

Funding

This research was funded by Fundação de Amparo à Pesquisa do Estado de Minas Gerais (FAPEMIG APQ-01674-18) and Conselho Nacional de Desenvolvimento Científico e Tecnológico (CNPq 311302/2020-3).

ORCID ID and Email

Victor Cardoso Campideli

victor.campideli@aluno.ufop.edu.br

<https://orcid.org/0000-0001-6262-2268>

Jerica Margely Montilla-Suárez

jerica.suarez@aluno.ufop.edu.br

<https://orcid.org/0000-0001-6898-6652>

Tiago Almeida Silva

tiago.a.silva@ufv.br

<https://orcid.org/0000-0002-7202-789X>

Dalila Chaves Sicupira

dalila@ufop.edu.br

<https://orcid.org/0000-0003-2552-6845>

Katia Mara Oliveira

katia.oliveira@unb.br

<https://orcid.org/0000-0003-4749-0281>

Rodrigo Souza Correa

rodrigocorrea@ufop.edu.br

<https://orcid.org/0000-0003-2783-0816>

References

- Cross, D.; Burmester, J. K. Gene therapy for cancer treatment: past, present and future. *Clin. Med. Res.* **2006**, *4*, 218–227.
- Kumar, L. S.; Prasad, K. S.; Revanasiddappa, H. D. Synthesis, characterization, antioxidant, antimicrobial, DNA binding and cleavage studies of mononuclear Cu(II) and Co(II) complexes of 3-hydroxy-N'-(2-hydroxybenzylidene)-2-naphthohydrazide. *Eur. J. Chem.* **2011**, *2*, 394–403.
- Rosenberg, B.; Vancamp, L.; Krigas, T. Inhibition of cell division in *Escherichia coli* by electrolysis products from a platinum electrode. *Nature* **1965**, *205*, 698–699.
- Clarke, M. J.; Zhu, F.; Frasca, D. R. Non-platinum chemotherapeutic metallopharmaceuticals. *Chem. Rev.* **1999**, *99*, 2511–2534.
- Mukhtar, S. D.; Suhail, M. Chiral metallic anticancer drugs: A brief review. *Eur. J. Chem.* **2022**, *13*, 483–490.
- Palchadhuri, R.; Hergenrother, P. J. DNA as a target for anticancer compounds: methods to determine the mode of binding and the mechanism of action. *Curr. Opin. Biotechnol.* **2007**, *18*, 497–503.
- Reedijk, J.; Lohman, P. H. Cisplatin: synthesis, antitumour activity and mechanism of action. *Pharm. Weekbl. Sci.* **1985**, *7*, 173–180.
- Rehman, S. U.; Sarwar, T.; Husain, M. A.; Ishqi, H. M.; Tabish, M. Studying non-covalent drug-DNA interactions. *Arch. Biochem. Biophys.* **2015**, *576*, 49–60.
- El-Shekeil, A. G.; Abubakr, A. O.; Al-Aghbari, S. A.; Nassar, M. Y. Anticancer 4: Anticancer and DNA cleavage studies of some new Schiff base titanium (IV) complexes. *Eur. J. Chem.* **2014**, *5*, 410–414.
- Geierstanger, B. H.; Wemmer, D. E. Complexes of the minor groove of DNA. *Annu. Rev. Biophys. Biomol. Struct.* **1995**, *24*, 463–493.
- Rupar, J.; Dobričić, V.; Brborić, J.; Čudina, O.; Aleksić, M. M. Square wave voltammetric study of interaction between 9-acridinyl amino acid derivatives and DNA. *Bioelectrochemistry* **2023**, *149*, 108323.
- Searle, M. S. NMR studies of drug—DNA interactions. *Prog. Nucl. Magn. Reson. Spectrosc.* **1993**, *25*, 403–480.
- Sirajuddin, M.; Ali, S.; Badshah, A. Drug-DNA interactions and their study by UV-Visible, fluorescence spectroscopies and cyclic voltammetry. *J. Photochem. Photobiol. B* **2013**, *124*, 1–19.
- Gonçalves, G. R.; de Carvalho, A. B.; Honorato, J.; Oliveira, K. M.; Correa, R. S. A new polymorph of six-coordinated bis(5,5'-dimethyl-2,2'-bipyridine) nitratocopper(II) nitrate and its DNA interactions. *J. Mol. Struct.* **2021**, *1224*, 129035.
- Oliveira, K. M.; Honorato, J.; Gonçalves, G. R.; Cominetti, M. R.; Batista, A. A.; Correa, R. S. Ru(II)/diclofenac-based complexes: DNA, BSA interaction and their anticancer evaluation against lung and breast tumor cells. *Dalton Trans.* **2020**, *49*, 12643–12652.
- Hartertinger, C. G.; Timerbaev, A. R.; Keppler, B. K. Capillary electrophoresis in anti-cancer metallodrug research: advances and future challenges. *Electrophoresis* **2003**, *24*, 2023–2037.
- Barolli, J.; Corrêa, R.; Miranda, F.; Ribeiro, J.; Bloch, C., Jr; Ellena, J.; Moreno, V.; Cominetti, M.; Batista, A. Polypyridyl ruthenium complexes: Novel DNA-intercalating agents against human breast tumor. *J. Braz. Chem. Soc.* **2017**, *28*, 1879–1889.
- Oliveira, K. M.; Honorato, J.; Demidoff, F. C.; Schultz, M. S.; Netto, C. D.; Cominetti, M. R.; Correa, R. S.; Batista, A. A. Lapachol in the design of a new ruthenium(II)-diphosphine complex as a promising anticancer metallodrug. *J. Inorg. Biochem.* **2021**, *214*, 111289.
- Oliveira, K. M.; Peterson, E. J.; Carroccia, M. C.; Cominetti, M. R.; Deflon, V. M.; Farrell, N. P.; Batista, A. A.; Correa, R. S. Ru(II)-Naphthoquinone

- complexes with high selectivity for triple-negative breast cancer. *Dalton Trans.* **2020**, 49, 16193–16203.
- [20]. Carvalho, D. E. L.; Oliveira, K. M.; Bomfim, L. M.; Soares, M. B. P.; Bezerra, D. P.; Batista, A. A.; Correa, R. S. Nucleobase derivatives as building blocks to form Ru(II)-based complexes with high cytotoxicity. *ACS Omega* **2020**, 5, 122–130.
- [21]. Graminha, A. E.; Popolin, C.; Honorato de Araujo-Neto, J.; Correa, R. S.; de Oliveira, K. M.; Godoy, L. R.; Vegas, L. C.; Ellena, J.; Batista, A. A.; Cominetti, M. R. New ruthenium complexes containing salicylic acid and derivatives induce triple-negative tumor cell death via the intrinsic apoptotic pathway. *Eur. J. Med. Chem.* **2022**, 243, 114772.
- [22]. da Silva, M. M.; Ribeiro, G. H.; de Camargo, M. S.; Ferreira, A. G.; Ribeiro, L.; Barbosa, M. I. F.; Deflon, V. M.; Castelli, S.; Desideri, A.; Corrêa, R. S.; Ribeiro, A. B.; Nicoletta, H. D.; Ozelin, S. D.; Tavares, D. C.; Batista, A. A. Ruthenium(II) diphosphine complexes with mercapto ligands that inhibit topoisomerase IB and suppress tumor growth in vivo. *Inorg. Chem.* **2021**, 60, 14174–14189.
- [23]. Bautista, M. T.; Cappellani, E. P.; Drouin, S. D.; Morris, R. H.; Schweitzer, C. T.; Sella, A.; Zubkowski, J. Preparation and spectroscopic properties of the η^2 -di-hydrogen complexes $[\text{M}(\eta^2\text{-H}_2)\text{PR}_2\text{CH}_2\text{CH}_2\text{PR}_2]_2$ + (M = iron, ruthenium; R = Ph, Et) and trends in properties down the iron group triad. *J. Am. Chem. Soc.* **1991**, 113, 4876–4887.
- [24]. Sheldrick, G. M. Crystal structure refinement with SHELXL. *Acta Crystallogr. C Struct. Chem.* **2015**, 71, 3–8.
- [25]. Macrae, C. F.; Bruno, I. J.; Chisholm, J. A.; Edgington, P. R.; McCabe, P.; Pidcock, E.; Rodriguez-Monge, L.; Taylor, R.; van de Streek, J.; Wood, P. A. Mercury CSD 2.0– new features for the visualization and investigation of crystal structures. *J. Appl. Crystallogr.* **2008**, 41, 466–470.
- [26]. Seda, S. H.; Abdel Aziz, A. A. Synthesis, spectral characterization, antimicrobial, DNA binding and antioxidant studies of Co(II), Ni(II), Cu(II) and Zn(II) metal complexes of novel thiosalen analog N2S2. *Eur. J. Chem.* **2015**, 6, 189–198.
- [27]. Vedanayaki, S.; Jayaseelan, P. Synthesis, structural characterization and biological properties of Cu(II), Ni(II), Mn(II), Zn(II) and VO(II) complexes of tetradentate Schiff bases. *Eur. J. Chem.* **2016**, 7, 368–374.
- [28]. Correa, R. S.; Freire, V.; Barbosa, M. I. F.; Bezerra, D. P.; Bomfim, L. M.; Moreira, D. R. M.; Soares, M. B. P.; Ellena, J.; Batista, A. A. Ru(II)-thymine complexes: new metallodrug candidates against tumor cells. *New J. Chem.* **2018**, 42, 6794–6802.
- [29]. Shi, J.-H.; Chen, J.; Wang, J.; Zhu, Y.-Y. Binding interaction between sorafenib and calf thymus DNA: spectroscopic methodology, viscosity measurement and molecular docking. *Spectrochim. Acta A Mol. Biomol. Spectrosc.* **2015**, 136 Pt B, 443–450.
- [30]. Tse, W. C.; Boger, D. L. A fluorescent intercalator displacement assay for establishing DNA binding selectivity and affinity. *Acc. Chem. Res.* **2004**, 37, 61–69.
- [31]. Sullivan, B. P.; Meyer, T. J. Comparisons of the physical and chemical properties of isomeric pairs. 2. Photochemical, thermal and electrochemical cis-trans isomerizations of $\text{M}(\text{Ph}_2\text{PCH}_2\text{PPh}_2)_2\text{Cl}_2$ (M = RuII, OsII). *Inorg. Chem.* **1982**, 21, 1037–1040.
- [32]. Lu, X.; Zhu, K.; Zhang, M.; Liu, H.; Kang, J. Voltammetric studies of the interaction of transition-metal complexes with DNA. *J. Biochem. Biophys. Methods* **2002**, 52, 189–200.
- [33]. Barbosa, M. I. F.; Corrêa, R. S.; de Oliveira, K. M.; Rodrigues, C.; Ellena, J.; Nascimento, O. R.; Rocha, V. P. C.; Nonato, F. R.; Macedo, T. S.; Barbosa-Filho, J. M.; Soares, M. B. P.; Batista, A. A. Antiparasitic activities of novel ruthenium/lapachol complexes. *J. Inorg. Biochem.* **2014**, 136, 33–39.
- [34]. Dinelli, L. R.; Batista, A. A.; Wohnrath, K.; de Araujo, M. P.; Queiroz, S. L.; Bonfadini, M. R.; Oliva, G.; Nascimento, O. R.; Cyr, P. W.; MacFarlane, K. S.; James, B. R. Synthesis and characterization of $[\text{RuCl}_3(\text{P-P})(\text{H}_2\text{O})]$ complexes; P-P = achiral or chiral, chelating ditertiary phosphine ligands. *Inorg. Chem.* **1999**, 38, 5341–5345.
- [35]. Polam, J. R.; Porter, L. C. Ru(II) Complexes containing chelating phosphine ligands. Synthesis, characterization, and X-ray crystal structures of dichlorobis(1,2-bis(diphenylphosphino)ethane)Ru(II) and the coordinatively unsaturated trigonal-bipyramidal cation, chlorobis-(1,2-bis(diphenylphosphino)ethane)Ru(II). *J. Coord. Chem.* **1993**, 29, 109–119.
- [36]. Lobana, T. S.; Singh, R.; Tiekink, E. R. T. The crystal and molecular structure of bis[1,2-bis(diphenylphosphino)ethane] dichloro ruthenium(II). *J. Coord. Chem.* **1990**, 21, 225–229.
- [37]. Chang, C.-W.; Ting, P.-C.; Lin, Y.-C.; Lee, G.-H.; Wang, Y. Synthesis of ruthenium vinylidene complexes with dppe ligand and their cyclopropanation reaction. *J. Organomet. Chem.* **1998**, 553, 417–425.
- [38]. Foi, A.; Corrêa, R. S.; Ellena, J.; Doctorovich, F.; Di Salvo, F. Halogen...halogen contacts for the stabilization of a new polymorph of 9,10-dichloroanthracene. *J. Mol. Struct.* **2014**, 1059, 1–7.



Copyright © 2023 by Authors. This work is published and licensed by Atlanta Publishing House LLC, Atlanta, GA, USA. The full terms of this license are available at <http://www.eurjchem.com/index.php/eurjchem/pages/view/terms> and incorporate the Creative Commons Attribution-Non Commercial (CC BY NC) (International, v4.0) License (<http://creativecommons.org/licenses/by-nc/4.0>). By accessing the work, you hereby accept the Terms. This is an open access article distributed under the terms and conditions of the CC BY NC License, which permits unrestricted non-commercial use, distribution, and reproduction in any medium, provided the original work is properly cited without any further permission from Atlanta Publishing House LLC (European Journal of Chemistry). No use, distribution, or reproduction is permitted which does not comply with these terms. Permissions for commercial use of this work beyond the scope of the License (<http://www.eurjchem.com/index.php/eurjchem/pages/view/terms>) are administered by Atlanta Publishing House LLC (European Journal of Chemistry).